An X-Ray diffraction (XRD) study to characterize the mineralogy of dinosaur bones from Arcillas de Morella Formation

Estudio de difracción de Rayos-X (DRX) para caracterizar la mineralogía de huesos de dinosaurio de la Formación Arcillas de Morella

Giampaolo Piga [1,4], Andrés Santos Cubedo [2], Massimo Piccinini [3] and Stefano Enzo [4]

[1] Unitat de Antropologia Biologica, Departament de Biologia Animal, Biologia Vegetal i Ecologia, Universitat Autonoma de Barcelona. E-08193 Bellaterra, Spain. kemiomara@yahoo.it
[2] Escuela Taller de Restauración Paleontológica IV, Departamento de Educación, Universidad, Cultura y Deporte del Gobierno de Aragón. Edificio Dinópolis, Avda. Sagunto s/n, E-44002 Teruel, Spain. santos.cubedo@gmail.com
[3] Porto Conte Ricerche Srl, Loc. Tramariglio, I-07041 Alghero-Sassari, Italy. piccinini@portocontericerche.it
[4] Dipartimento di Chimica, Università di Sassari. via Vienna 2, I-07100 Sassari, Italy. enzo@uniss.it

ABSTRACT

An investigation by powder X-ray Diffraction (XRD), supplemented with the Rietveld analysis, was conducted on twenty-two Spanish dinosaur bone specimens from Lower Cretaceous age to investigate mineralogy, taphonomy and diagenetic processes. The diffraction approach assessed in all specimens the presence of fluorapatite at various levels of percentage as the mineral phase constituting the fossil bone. In addition to fluorapatite, calcite and quartz were also found as main secondary phases in many specimens. The average crystallite size of the "apatitic" constituent phase was found to vary from a minimum of ca. 183 Å to an upper level of 2107 Å. No systematic relation between apatite crystallite size and age of the dinosaur bones was found that suggests a high variability of diagenetic processes affecting the growth of bone crystallites even in the same site.

Key-words: *X-ray Diffraction, dinosaur bones, mineralogy, diagenetic processes.*

RESUMEN

Se ha realizado el análisis de difracción de rayos X (DRX), complementado con Rietveld, en veintidós muestras de huesos de dinosaurios del Cretácico Inferior para investigar la mineralogía y los procesos diagenéticos y tafonómicos. El estudio de difracción da como resultado la presencia de fluorapatito en distintos niveles de porcentaje, como la principal fase mineral que constituye el hueso fósil. Además del fluorapatito, se ha encontrado calcita y cuarzo como principales fases secundarias. El tamaño de los cristales de la fase "apatítica" va desde un mínimo de ca. 183 Å a 2107 Å. No se ha encontrado ninguna relación entre el tamaño de los cristales de apatito y la edad de los huesos de dinosaurio, lo que sugiere una alta variabilidad en los procesos diagenéticos que afectan al crecimiento de los cristales, incluso dentro del mismo yacimiento.

Palabras clave: *Difracción de rayos-X, huesos de dinosaurios, mineralogía, procesos diagenéticos.*

Geogaceta, 51 (2012), 23-26.
ISSN:2173-6545

Fecha de recepción: 15 de Julio de 2011
Fecha de revisión: 3 de noviembre de 2011
Fecha de aceptación: 25 de noviembre de 2011

Introduction

Chemical and mineralogical studies are mainly focused on archaeological samples and biomaterials and only to a little extent on dinosaur fossils (Piga *et al.*, 2011 and references therein). Changes involving the structure and chemical composition of bones may occur in two different periods, i.e., first during the animal's life, and second during the fossilization process. The time scale of these two stages may be incommensurable and a distinction is made between biostratinomy and fossildiagenesis.

Some processes may occur to preserve rather than degrading fossils, particularly the incorporation of new ions into the crystal structure and/or recrystallisation of skeletal apatite. These processes are mainly controlled by abiotic, physical and chemical environmental soil conditions, particularly groundwater chemistry around the buried bone material (Trueman *et al.*, 2004; Tütken *et al.*, 2008). The bioapatite of animal and human bones turns out to be very similar at an atomic level and the structure is generally approximated using the stoichiometric mineral hydroxylapatite $Ca_5(PO_4)_3OH$.

A good knowledge of the chemical and mineralogical composition of fossil bones as the result of a whole host of physical, chemical and biological processes can be obtained directly from fluorescence and powder diffraction of X-rays (Bradley *et al.*, 2007). The recent numerical development of powder X-ray Diffraction technique according to the Rietveld method has supplied a new approach to reveal the structure details of natural apatites, as we have recently verified in archaeological and geological contexts (Piga *et al.*, 2009; Piga *et al.*, 2011).

A XRD approach proved to be useful to better characterize the mineralogical and chemical composition of fossil bones. Herein we analyze the mineralogy of dinosaur bones to a better understanding of bone fossilization processes, because this is important, for example, in order to choose the appro-

priate treatment and chemical products for optimal conservation and preservation of the fossils.

Materials and methods

Twenty-two dinosaur bone samples (Lower Cretaceous, Arcillas de Morella Formation) belonging to dinosaurs of different taxa are studied.

The vertebrate material was mechanically separated from the sediment with an engraver drill. Subsequently the bones were washed with distilled water. For all specimens, the bone was sampled in the innermost part of the bone cortex (compacta) of the cortical tissue.

Bone samples were kindly made available from the Colección Museográfica de Cinctorres (Castellón). For comparison to the fossil dinosaur bone samples a modern animal bone as well as synthetic hydroxylapatite was also analyzed using the same techniques. The modern bone of a rhesus monkey was made available by Teesside University (Middlesbrough, UK); synthetic powder hydroxylapatite was synthesized by Aldrich chemistry®.

0.5 g of each dinosaur bone was ball milled in an agate jar for one-minute using a SPEX mixer-mill model 8000. Our sample holder for XRD analysis is a circular cavity of 25 mm in diameter and 3 mm in depth. It contains about 420 mg of powder.

The XRD patterns were recorded overnight using Bruker D8, Philips PW-1050 and Siemens D-500 diffractometers in the Bragg–Brentano geometry with CuK radiation (λ1.54178 Å). The X-ray generator worked at a power of 40 kV and 30 mA and the resolution of the instruments (divergent and antiscatter slits of 0.5°) was determined using -SiO_2 and -Al_2O_3 standards free from the effect of reduced crystallite size and lattice defects (Enzo *et al.*, 1988).

The goniometer was equipped with a graphite monochromator in the diffracted beam and the patterns were collected with 0.05° of step size which turned out to be adequate for the range of crystallite size in apatite phases here investigated. The powder patterns were collected in the angular range 10°-140° in 2 , with counting time of 40 s per point. Digitized diagrams were analyzed according to the Rietveld method (Rietveld, 1967), using the programme MAUD (Lutterotti *et al.*, 1998). For inorganic phase mixtures of medium complexity (3-4 phases) the detection limit of the technique is thought to be 1-2 wt%. One advantage of the Rietveld method is that no standard is required for quantitative evaluation of phases, thus minimizing the work on sample preparation. Moreover, one merit of the MAUD program is that the numerical evaluation of the whole pattern is accomplished using all recognized phases with a parametric peak shape function convoluting the instrument function with simultaneous broadening due to size and strain effects.

XRF inspects the phase composition. In addition to this, the line broadening analysis of XRD patterns may be applied for a simple evaluation of crystallinity in hydroxylapatite (HA), which is the main biomineral phase of bones. Note that the term crystallinity is instinctively intended as degree of organization of the bone HA phase on an atomic scale.

Rather than referring to the crystallinity of HA, a valid and more correct approach is to evaluate the X-ray peak sharpening of HA bones in terms of the average size of coherently diffracting domains (otherwise referred to as crystallites) and/or average imperfection density, also called lattice disorder or microstrain (Hubert *et al.*, 1996). These parameters supply a means to define numerically the organization of bones in an atomic scale. The quantitative evaluation of phases, their lattice parameters and their average coherent diffraction domain size may be obtained by applying the Rietveld method as it was suggested by Michel *et al.* (1995).

Results and discussion

Table I displays the main phases of dinosaur bones found by the XRD investigation with quantitative parameters estimated according to the Rietveld method, i.e., the cell volume of the supposed "apatitic" phase and its average crystallite size.

Concerning the phases constituting the fossil bones, a high variability can be pointed out among the various samples. The most frequent phases in the samples studied are mostly fluorapatite, quartz and calcite. The apatite phase content in the various specimens varies because of the number and amount of the other secondary mineral phases present, ranging from a minimum of 52 wt% for the sample Torre Julián, up to 100 wt% in the case of the samples Escapula Ana, 4ANA75 and Patiràs.

Quartz normally derives from the embedding sediment and rarely is an authigenic mineral. Conversely, the presence of calcite as an authigenic mineral is common in many fossil sites (Hubert *et al.*, 1996; Astibia *et al.*, 2005) and may infill bone voids or precipitate at the surface as a thin white crust. Our evidence at a micro-scale level from confocal Raman shows that calcite occupies the haversian canals.

In other studied specimens we have also determined other phases such as kaolinite (25 wt% [$Al_2Si2O_5(OH)_4$], Povet), goethite (28 wt% FeOOH, A10), and berlinite (1 wt% $AlPO_4$, SAV 67 specimen).

The molar volume VM/2 of each monoclinic cell of the apatite-like phase is varying from a lower value of 522.5 $Å^3$ (A13) to an upper value of 525.7 $Å^3$ (Comptadors-A1). This is consistent with the literature data referred to fluorapatite that supply several unit cell volume values ranging from 522.18 $Å^3$ to 528.41 $Å^3$, respectively (McConnell, 1973; Hughes *et al.*, 1989).

Even the literature values of francolite range from a minimum of 518.73 $Å^3$ to a maximum of 523.81 $Å^3$ (Sudarsanan and Young, 1978) and scatter around the values reported for fluorapatite. We have recently estimated that fluorination of bone apatite is taking place in about 4-5 Ma after examining the unit cell volume change of biogenic apatite vs. geological age (Piga *et al.*, 2009).

However, we have previously observed (Piga *et al.*, 2009) that the recrystallization process brought about by fossilization does not occur homogeneously across geological times. For example, for the Camino and EAP 40-39 specimens, we have pointed out an evident difference in the peak broadening of the two patterns, on account of average crystallite size of 2107 Å (± 100 Å) and 382 Å (± 20 Å), respectively. Also, out of the three fossils consisting of single phase apatite examined in figure 1, the larger average crystallite size (ca. 410 ± 20 Å) is observed for the sample with the most recent stratigraphic age.

Figure 1, displays the XRD experimental patterns (data points) and the Rietveld fit (full lines) of three fossil specimens compared with a modern bone and with the hydroxylapatite mineral synthesized chemically in the laboratory.

The patterns of these specimens, namely Escapula Ana, 4ANA75 and Patiras are single phase because satisfactorily described using the structure factor of monoclinic apatite, precisely fluorapatite. Following Elliott *et al.* (1973) we have adopted a monoclinic description of the unit cell (Space Group P21/c,

Sample code	Phase wt %	Average crystallite size (Å) (±5%)	a/ Å (±0.001)	b/Å (±0.002)	c/ Å (±0.001)	g/° (±0.05)	Vc/2 /Å^3 (±0.3)
Patiras	Apatite 100%	420	9.3481	18.796	6.897	120.12	524.1
SAV-39	Apatite 96% Quartz 4%	399	9.357	18.808	6.896	120.14	524.8
SAV-67	Apatite 85% Quartz 7% Berlinite 1% Kaolinite 7%	457	9.363	18.817	6. 897	120.16	525.3
Povet	Apatite 67% Kaolinite 25% Quartz 8%	437	9.372	18.735	6.899	120.10	524.0
Camino	Apatite 80% Calcite 20%	2107	9.377	18.748	6.894	120.02	524.7
EAP 38	Apatite 94% Calcite 1% Goethite 4% Quartz 1%	352	9.344	18.787	6.895	120.06	523.8
EAP 40-39	Apatite 88% Calcite 12%	382	9.348	18.781	6.895	120.05	523.9
EAP 43	Apatite 93% Calcite 3% Quartz 3% Goethite 1%	485	9.345	18.796	6.894	120.00	524.3
Compta dors A1	Apatite 66% Calcite 24% Quartz 8% Kaolinite 2%	432	9.365	18.822	6.896	120.13	525.7
Todolcell a 1	Apatite 98% Calcite 1% Quartz 1%	436	9.365	18.823	6.894	120.16	525.4
Torre Julian	Apatite 52% Calcite 47 % Quartz 1%	411	9.340	18.738	6.901	119.75	524.3
A 10	Apatite 68% Quartz 4% Goethite 28%	226	9.355	18.757	6.896	120.25	522.6
A 13	Apatite 96% Quartz 2% Goethite 2%	255	9.341	18.759	6.895	120.12	522.5
2ANA12	Apatite 96% Calcite 4%	282	9.349	18.776	6.895	120.11	523.5
2ANA61	Apatite 82% Quartz 14% Goethite 4%	310	9.334	18.764	6.902	119.80	524.5
2ANA77	Apatite 92% Calcite 4% Goethite 3% Quartz 1%	298	9.392	18.735	6.896	120.25	524.1
3ANA58	Apatite 88% Calcite 5% Goethite 4% Quartz 3%	274	9.357	18.721	6.902	119.92	524.0
4ANA3	Apatite 68% Quartz 22% Goetite 8%	183	9.340	18.741	6.895	119.85	523.4
4ANA75	Apatite 100%	312	9.353	18.740	6.893	120.05	522.9
Escápula -ANA	Apatite 99% Calcite 1%	278	9.376	18.815	6.901	120.30	525.6
Mas Roig	Apatite 75% Calcite 3% Kaolinite 22%	347	9.378	18.741	6.904	120.14	524.7
Mas dc Rafael-2	Apatite 91 % Calcite 9%	311	9.352	18.739	6.892	119.96	523.2

Table I.- List of the XRD phase analysis of the dinosaur bones complemented with average crystallite size and lattice parameters cell volume of monoclinic apatite structure data.

Tabla I.- Listado del análisis de DRX de las fases presentes en los huesos de dinosaurios complementados con el tamaño de cristalito promedio y el volumen de la celda unidad de la estructura monoclínica del apatito.

4 molecular units) rather than the usual hexagonal cell of S. G. P63/m with two molecules of hydroxylapatite because this appears to be more stable from an energetic point of view. As a matter of fact, the lattice parameter of the monoclinic phase aM (M refers to monoclinic) coincides with that of the hexagonal phase aH (H stands for hexagonal), but bM is about 2×aH, cM=cH and bM≈120° (Ikoma *et al.*, 1999). Thus, the monoclinic unit cell volume VM is about twice that of VH.

Despite the care used in the fossil unearthing procedure, cleaning and sampling the compact part of the bone, the possibility of the incorporation of clay minerals in the internal pore space of buried fossil bones is always very likely, as demonstrated by the results of the Povet specimen.

The XRD pattern is described in terms of apatite component, accompanied by a large fraction of kaolinite and some quartz. Both kaolinite and quartz can be ascribed to the most common minerals of embedding sediment and were likely incorporated into the bone pore space.

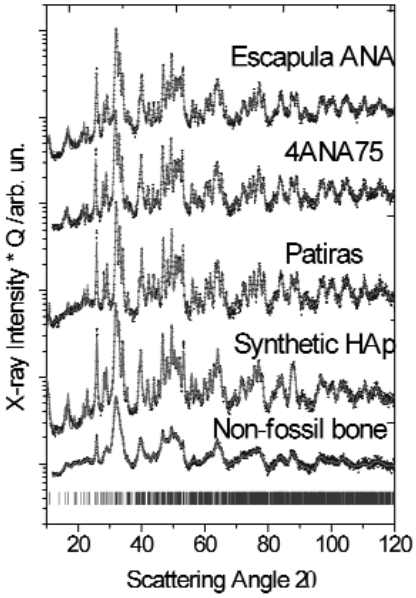

Fig. 1.- A comparison of XRD spectra of a modern animal bone (bottom), synthetic apatite, and three dinosaur single-phase (fluorapatite) bones.

Fig. 1.- Comparación del difractograma del hueso de una animal moderno (abajo), apatito sintético y tres huesos de dinosaurios compuestos por una sola fase (fluorapatito).

The XRD pattern refinement of the A10 specimen is not anymore single-phase. As reported in the Table I, the apatite-like phase is the most abundant, but is accompanied by ca. 28 wt% of goethite and small

quantity of quartz. The presence of goethite was also reported previously in other dinosaur bones (Elorza *et al.*, 1999), though not evaluated quantitatively, and was attributed to a hydromorphic process because of seasonal variations of the phreatic water level.

An important issue concerns the variability of phase and chemical composition of bone specimens from the same geological setting. This comparison is reported in figure 2, which shows the XRD pattern of specimens Camino and EAP 40-39.

The upper pattern referred to the

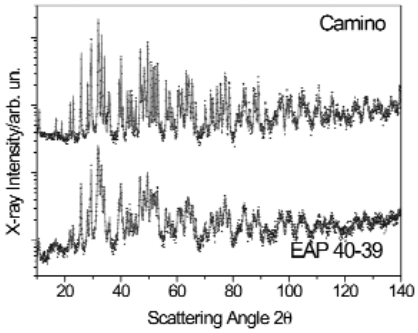

Fig. 2.- The upper pattern referred to the Camino shows line profiles from the FA sharper than in the EAP 40-39, on account of markedly different average crystallite size.

Fig. 2.- El difractograma superior, Camino, muestra una línea de FA más definida que EAP 40-39, debido a una marcada diferencia en el tamaño de cristalito promedio.

Camino specimen shows line profiles from the fluorapatite sharper than in the EAP 40-39 specimen at the bottom, reflecting a markedly different average crystallite size. This comparison may be better evaluated across a narrower angular 2θ range (30°-60°) as reported in the plot of figure 3.

The unpredictable change of the average crystallite size values and SFs suggest that correlation between crystallisation indices and bone age has to be regarded with obvious caution, as it was suggested by Person *et al*. (1995) and Farlow and Argast (2006).

In our previous study (Piga *et al.*, 2009), we observed a positive correlation between average bone apatite crystal size and specimen age in another set of fossils ranging in age from the Middle Triassic (around 245 Ma) to present. It seems that the crystallization induced by just the time is overlapped by other factors depending on the geological formation that may inhibit (e.g., 4ANA3 sample) or enhance the process.

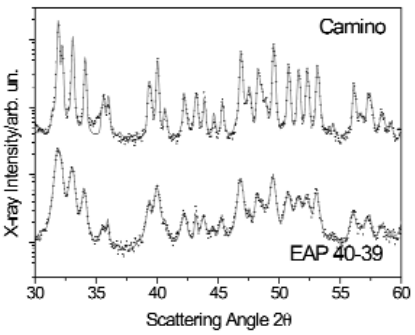

Fig. 3.- Better comparison across a narrower angular range reported in the figure 2.

Fig. 3.- Mejor comparación del rango angular que el reportado en la figura 2.

The Camino specimen stands out of any general trend as an outlier since we do not observe an apatite crystallize size that exceeds 485 Å (EAP 43 specimen) for all other dinosaur bone specimens. Beyond diagenesis the large crystallite size of ca. 2000 Å might be the result of fire exposure to which this dinosaur bone was possibly subjected. In fact, similar high values for the average apatite crystallite size have been reported only for human bones incinerated in a temperature range of 900-1000 °C (Piga *et al.*, 2008).

Conclusions

From the crystal lattice parameters of the apatite phase determined by powder XRD, it emerged that these fossil bones invariably underwent a post-mortem transformation from bioapatite (hydroxylapatite) to authigenic fluorapatite structure. For a large number of specimens the presence of secondary quartz and calcite phases were frequently observed while goethite and kaolinite were found in various specimens. The average crystallite size of the apatite-like phase ranges from 183 Å to 2107 Å and varies unpredictably in the analysed specimens, inhibiting a correlation with fossil age.

Acknowledgements

The authors thank: Prof. Assumpció Malgosa (UAB), Prof. Salvador Moyà Solà (ICP). Special thanks to Prof. Carlos de Santisteban and one anonymous reviewer for their helpful comments on the manuscript. This study is partially supported by PR1-MAB-A2008-443 (Autonomous Region of Sardinia) and CGL2008-06533-C03-03/BTE (Spanish M. of Science and Innovation).

References

Astibia, H., Payros, A., Suberbiola, X., Berreteaga, A., Elorza, J., Extebarria, N. and Tosquella, J. (2005). *Facies*, 50, 463-475.

Bradley, D.A., Muthuvelu, P., Ellis, R.E., Green, E.M., Attenburrow, D., Barrett, R., Arkill, K., Colridge, D.B. and Winlove, C.P. (2007). *Nuclear Instruments and Methods in Physics Research B*, 263, 1-6.

Elliott, J.C., Mackie, P.E. and Young, R.A. (1973). *Science*, 180, 1055-1057.

Elorza, J., Astibia, H., Murelaga, X. and Pereda-Suberbiola, X. (1999). *Cretaceous Research*, 20, 169-187.

Enzo, S., Fagherazzi, G., Benedetti, A. and Polizzi, S. (1988). *Journal of Applied Crystallography*, 21, 536-542.

Farlow, J.O. and Argast A. (2006). *Journal of the Paleontological Society of Korea*, 22, 51-75.

Hubert, J.F., Panish, P.T., Chure, D.J. and Prostak, K.S. (1996). *Journal of Sedimentary Research*, 66, 531-547.

Hughes, J.M., Cameron, M. and Crowley, K.D. (1989). *American Mineralogist*, 74, 870-876.

Ikoma, T., Yamazakai, A., Nakamura, S. and Akao, M. (1999). *Journal of Solid State Chemistry*, 144, 272-276.

Lutterotti, L., Ceccato, R., Dal Maschio, R. and Pagani, E. (1998). *Materials Science Forum*, 2, 87-92.

McConnell, D. (1973). *Apatite; its crystal chemistry, mineralogy, utilization, and geologic and biologic occurrences*. Springer-Verlag. 111 p.

Michel, V., Ildefonse, Ph. and Morin, G. (1995). *Applied Geochemistry*, 10, 145–159.

Person, A., Bocherens, H., Saliege, J.F., Paris, F., Zeitoun, V. and Gerard, M. (1995). *Journal of Archaeological Science*, 22, 211-221.

Piga, G., Malgosa, A., Thompson, T.J.U. and Enzo, S. (2008). *Journal of Archaeological Science*, 35, 2171-2178.

Piga, G., Santos-Cubedo, A., Moya Solà, S., Brunetti, A., Malgosa, A. and Enzo, S. (2009). *Journal of Archaeological Science*, 36, 1857-1868.

Piga G., Santos-Cubedo A., Brunetti A., Piccinini M., Napolitano E., Malgosa A. and Enzo S. (2011). *Palaeogeography, Palaeoclimatology, Palaeoecology*, 310, 92-107.

Rietveld, H.M. (1967). *Acta Crystallographica*, 22, 151-152.

Sudarsanan, K. and Young, R.A. (1978). *Acta Crystallographica*, B34, 1401-1407.

Trueman, C.N.G., Behrensmeyer, A.K., Tuross, N. and Weiner, S. (2004). *Journal of Archaeological Science*, 31, 721-739.

Tütken, T., Vennemann, T.W. and Pfretzschner, H.U. (2008). *Palaeogeography, Palaeoclimatology, Palaeoecology*, 266, 254–268.